DEUTSCHES ELEKTRONEN – SYNCHROTRON

INSTITUT FÜR HOCHENERGIEPHYSIK

DESY 92-027
February 1992

Multiplicity Structure of Inclusive Diffraction in pi^+p and K^+p Interactions at 250 GeV/c

The EHS/NA22 Collaboration

ISSN 0418-9833

PLATANENALLEE 6 · O-1615 ZEUTHEN

To be sure that your preprints are promptly included in the HIGH ENERGY PHYSICS INDEX, send them to the following (if possible by air mail):

DESY Bibliothek Notkestraße 85 W-2000 Hamburg 52 Germany	DESY-IfH Bibliothek Platanenallee 6 O-1615 Zeuthen Germany

DESY 92-027
February 1992

ISSN 0418-9833

MULTIPLICITY STRUCTURE OF INCLUSIVE DIFFRACTION IN π^+p and K^+p INTERACTIONS AT 250 GeV/c

EHS/NA22 Collaboration

M.BEGALLI[1], F.BOTTERWECK[2], H.BOETTCHER[3], M.CHARLET[2a], P.V.CHLIAPNIKOV[4], E.A.De WOLF[5b], K.DZIUNIKOWSKA[6], A.M.F.ENDLER[1], A.ESKREYS[6], W.FRIEBEL[3], G.R.GULKANYAN[7], Z.S.GARUTCHAVA[8], W.KITTEL[2], S.S.MEGRABYAN[7], Th.NAUMANN[3], K.OLKIEWICZ[5], H.E.ROLOFF[3], O.G.TCHIKILEV[4], L.A.TIKHONOVA[9], A.G.TOMARADZE[8], F.VERBEURE[5], R.WISCHNEWSKI[3], S.A.ZOTKIN[9].

[1] Centro Brasileiro de Pesquîsas Fisicas, 22290 Rio de Janeiro, Brazil
[2] University of Nijmegen and NIKHEF-H, NL-6525 ED Nijmegen, The Netherlands
[3] DESY - Institut für Hochenergiephysik, D-O-1615 Zeuthen, Germany
[4] Institute for High Energy Physics, SU-142284 Protvino, Russia
[5] Inter-University Institute for High Energies, B-1050 Brussels and Universitaire Instelling Antwerp, B-2610 Wilrijk, Belgium
[6] Institute of Physics and Nuclear Technique of the Academy of Mining and Metallurgy and Institute of Nuclear Physics, PL-30055 Krakow, Poland
[7] Institute of Physics, SU-375036 Yerevan, Armenia
[8] Institute for High Energy Physics, Tbilisi-State University, SU-380086 Tbilisi, Georgia
[9] Nuclear Physics Institute, Moscow State University, SU-119899 Moscow, Russia

Abstract

Results on the multiplicity structure of diffractively excited meson and proton systems in π^+/K^+p interactions at 250 GeV/c are presented for diffractive masses up to about 9 GeV. The energy dependence of the average charge multiplicity and the shape of the multiplicity distribution in terms of KNO-scaling and Negative Binomial distribution are investigated. The diffractive systems are compared to e^+e^- , lh and non-diffractive hh final states as suggested by modern approaches of the Pomeron-hadron collision. Systematic differences are found between diffractive meson and proton systems but also between diffraction and the reactions compared to.

(to be submitted to Z.Phys.C)

[a] EC Guest Scientist
[b] Bevoegdverklaard Navorser NFWO, Belgium

1 Introduction

Recent experimental results on hadron diffraction [1-6] have confirmed an elongation of the diffractively excited hadron system along the Pomeron-hadron direction. Such an elongation rules out a fireball-like, isotropic decay, but is expected in parton-oriented models for diffraction. Currently, two phenomenological partonic approaches to the Pomeron-hadron interaction may be distinguished: one is the Pomeron-photon picture [7-12] where the Pomeron couples to single quarks as the photon in deep inelastic scattering, the other the Pomeron-meson picture [13-15] where the Pomeron interacts as a quark-antiquark pair.

According to the Pomeron-photon picture, the characteristics of diffractive hadron systems should be comparable with hadron production in semi-hard and hard processes. In the simplest case of scattering off a valence quark, one would expect an excitation of a quark-antiquark system in meson diffraction and of a quark-diquark system in proton diffraction, leading to similarities with e^+e^- annihilation into hadrons and with lepton-hadron collisions, respectively. The Pomeron-meson picture underlines a more hadronic character of the Pomeron, according to which the Pomeron-hadron interaction should be similar to non-diffractive hadron-hadron scattering.

An experimental distinction between the two pictures of Pomeron-hadron interaction is difficult since both concepts predict similarly elongated hadronic systems. Furthermore, the Pomeron-meson picture can be interpreted as scattering off a sea-quark and therefore as part of the Pomeron-photon picture. Common to both pictures is, however, that differences are expected between the properties of the (elongated) diffractive meson and proton systems.

In this paper we, therefore, concentrate on a detailed comparison of the multiplicity structure of meson and proton diffraction. Our diffrative data are further compared to data on hadron production in e^+e^- , lh and non-diffractive hh collisions.

The experimental data selection is briefly discussed in Sect. 2. Results on moments and on the shape of the multiplicity distributions are given in Sect. 3, with the comparison to e^+e^- , lh and non-diffractive hh data where appropriate. Sect. 4 summarizes the main results.

2 Experimental data

The experiment NA22 has been performed at the CERN SPS using the European Hybrid Spectrometer (EHS) equipped with the H_2 filled Rapid Cycling Bubble Chamber (RCBC) as an active vertex detector and exposed to a tagged positive meson enriched beam of 250 GeV/c, the highest beam momentum so far reached for positive meson-proton collisions. Details on the full experimental set-up and the minimum bias interaction trigger used in data taking are given elsewhere [16]. The 4π acceptance for charged particles in RCBC and the good momentum resolution over the whole momentum range ($< \Delta p/p > \sim 1.5\,\%$ in RCBC, $\sim 2.5\%$ at 30 GeV/c and $\sim 1.5\%$ at 100 GeV/c) are properties of EHS suitable to isolate and study the diffractive components.

For the present analysis, only well measured and reconstructed events with the proper charge balance are accepted. Identification of slow protons in the RCBC ($p_{lab} < 1.2$ Gev/c) is provided by a special ionization scan for 100 % of the K^+ and 70 % of the π^+ data. For the remaining 30 % of the π^+ sample the mass dependent fits in GEOHYB

(the EHS geometry program) are used. The mass of the beam particle is given to the fastest track if of positive charge and of momentum $p_{lab} > 120$ GeV/c. All other tracks are taken as pions. Elastic events are excluded from the analysis. All events are properly weighted to account for losses due to the interaction trigger, the reconstruction chain, and the proton identification. The experimental procedure used to obtain the inelastic event sample is identical to that described in [1], except for the addition of further information on particle identification. After these cuts we are left with 54032 inelastic π^+p and 19834 K^+p interactions representing our final statistics of well reconstructed inelastic events.

In selecting the diffractive components the same selection criteria are applied as in [1]. There, it has been shown that a cut in the backward and forward leading particle Feynman-x spectra ($x_F < -0.85$ for the backward and $x_F > 0.80$ for the forward leading particles, i.e. the slow proton and the fastest positively charged hadron, respectively), combined with a maximum-rapidity-gap cut ($\Delta y_{max} = 2.0$ between the leading and the next-to-leading particle) and an estimation of the non-diffractive background gives a rather clean isolation of meson and proton diffractive event samples, with clear signals for diffractive masses M_D up to about 9 GeV and charge multiplicities even above $n_{ch} = 8$. Finally, we obtain $5499\pi^+$ and $2252K^+$ events representing meson diffraction according to the reaction

$$\pi^+/K^+p \rightarrow \pi^+_D/K^+_D\,p. \qquad (1)$$

The proton diffractive event sample according to the reaction

$$\pi^+/K^+p \rightarrow \pi^+/K^+p_D \qquad (2)$$

consists of $4098\,\pi^+$ and $1411\,K^+$ events. Since differences between the π^+ and K^+ data are not relevant for our analysis, the event samples have been combined in order to increase statistics. In the following π^+_D/K^+_D denotes meson and p_D proton diffraction as already applied in (1) and (2).

3 Charge Multiplicities

3.1 Moments of the charge multiplicity distribution

The average charge multiplicity $< n^D_{ch} >$ of the diffractive meson and proton systems is presented in fig. 1a as a function of the diffractive mass M_D, where n^D_{ch} is given by $n^D_{ch} = n_{ch} - 1$. The difference between the meson and proton data observed in fig. 1a is reduced if instead of M_D the dependence on the available energy E_a is considered (fig. 1b). Here, E_a is defined as $E_a = M_D - m_{h^+}$, where h^+ refers to the incoming hadron π^+, K^+ or p. As can be seen, however, a significant difference remains. Except for the lowest energies, the diffractive meson system has a higher average multiplicity than the proton system. We note. that a similar difference has been observed between charge multiplicites in non-diffractive meson-proton and proton-proton interactions (see e.g. [16]). Both the meson and proton data can be well fitted by a polynomial quadratic in $ln\,M_D$ or $ln\,E_a$, respectively, as indicated by the lines in fig.1. The resulting fit parameters and the goodness of the fits are summarized in table 1.

The $< n^D_{ch} >$-values together with other moments of the multiplicity distribution, namly D, f_2 and the ratio $< n^D_{ch} > /D$, are collected in table 2 and 3 as a function of M_D. The errors include statistical as well as systematic uncertainties from estimation of the non-diffractive background. The dispersion D, the correlation parameter f_2 and the ratio

$< n^D_{ch} > /D$ are plotted as a function of M_D in fig.2. While D increases with increasing M_D, the ratio $< n^D_{ch} > /D$ stays approximately constant at least above $M_D \approx 3$ GeV with a somewhat higher level for meson than for proton diffraction. This indicates that meson diffractive multiplicity distributions are getting narrower than proton diffractive ones again in analogy with non-diffractive hadron-hadron interactions [16].

An investigation of the particle flow into the forward and backward hemispheres of the diffractive rest frame is in preparation and will be published in a forthcoming paper [17]. Following the discussion in the introduction, a comparison of the diffractive multiplicities to those of hadronic systems from hard and/or soft reactions is performed in figs. 3 and 4. In fig. 3 we compare the average charge multiplicity of meson diffraction and hadron production in e^+e^- annihilation [18] as a function of the energy $M_D = \sqrt{s}$ (see also [1]). Within the given experimental accuracy, a reasonable agreement can be seen in the region of overlap ($M_D \geq 3$ GeV). Higher average multiplicities in e^+e^- reactions are expected in a model for diffraction by Dias de Deus [12] which explores the Pomeron-photon picture.

Based on similar arguments concerning the hadronization of quark-diquark systems we present in fig. 4 a comparison of proton diffraction with deep inelastic lepton-hadron scattering [19]. From the total hadronic net-charge Q_H ($Q_H = 2$ for νp, $Q_H = 0$ for $\bar{\nu}p$ and $Q_H = 1$ for μ^+p) one would expect similarities with the μ^+p data. The general trend of the proton data is within errors compatible with μ^+p as well as with $\bar{\nu}p$ interactions. The νp points lie above the proton diffraction values throughout the energy range considered.

In fig. 5 we present the energy dependence of the ratio $< n_{ch} > /D$ for meson and proton diffraction and compare it with that for e^+e^- [18,20], μ^+p [19c], $M^{\pm}p$ [16, 21a,b,d,e] and $pp/p\bar{p}$ [16,21a,e,22] data, where $M^{\pm}$ denotes positively or negatively charged mesons. At high energies, the e^+e^- and the $pp/p\bar{p}$ data become independent of the energy and develop a sort of upper and lower limit for $< n_{ch} > /D$-values. The values for e^+e^- are about 50 % higher than those for $pp/p\bar{p}$. All other reactions do not reach this energy region, but seem to lie in between these two limits (see also [18e] and [19c]). At lower energies, a clear relationship between the different reaction types is smeared out. Concerning diffraction more data at higher energies are needed to clarify this point.

3.2 The shape of the multiplicity distribution

In studying the shape of the diffractive multiplicity distribution in more detail we restrict our analysis to diffractive masses M_D greater than 3 GeV, i.e. above the resonance region. The normalized multiplicity distributions for this mass region are given in tables 4 and 5 for meson and proton diffraction, respectively. In fig. 6 the meson diffractive data in the four highest mass intervals are plotted in their KNO-form

$$\psi(z) = < n_{ch} > P_{n_{ch}}, \qquad (3)$$

where $z = n_{ch}/ < n_{ch} >$ and $P_{n_{ch}}$ is the probability of the multiplicity n_{ch}. They are compared with hadron data from e^+e^- interactions at appropriate energies $M_D = \sqrt{s}$ [18b,c]. Although, within the experimental errors KNO-scaling seems to hold among the different data sets, indications for a small but significant difference between meson diffraction and e^+e^- data become visible when parameterising these data according to the one-parameter KNO-function [23]

$$\psi(z) = 2\,\frac{e^{-c}\,c^{cz+1}}{\Gamma(cz+1)}. \qquad (4)$$

The lines drawn in fig. 6 represent fits to the combined meson and combined e^+e^- data sets giving $c = 6.70 \pm 0.22$ with $\chi^2/NDF = 30.8/24$ for meson diffraction and $c = 7.71 \pm 0.20$ with $\chi^2/NDF = 11.4/18$ for hadron production in e^+e^- annihilations. The e^+e^- KNO-curve in fig.6 appears to be narrower than the meson curve.

In fig. 7 a similar comparison is performed between proton diffraction and hadron data in μ^+p interactions. Here again, one could conclude from the data points that KNO-scaling would hold. However, when fitting the combined proton and the combined μ^+p data separately with relation (4), a small but systematic difference appears, the μ^+p KNO-curve is narrower than the proton curve. The fit results are $c = 4.78 \pm 0.15$ with $\chi^2/NDF = 23.9/24$ for proton diffraction and $c = 6.00 \pm 0.22$ with $\chi^2/NDF = 26.2/17$ for hadron production in μ^+p interactions.

To study the energy dependence of the parameter c, the data sets have been fitted in the different energy intervals. The results are summarized in table 6 and compared with hadron production in e^+e^- [18b, c, e] and lp interactions ($\bar{\nu}p$ [19b], μ^+p [19c]) in fig. 8. The fits for the latter data sets have been done partly only on the basis of published KNO-plots. The energy dependence of the parameter c seems to be weak in the energy range considered at least for the diffractive data (approximate KNO-scaling). Clearly, diffractive data at higher energies are needed.

The results of a fit of the diffractive multiplicity distributions by the Negative Binomial distribution

$$P_n(\bar{n},k) = \binom{n+k-1}{k-1} \frac{(\bar{n}/k)^n}{(1+\bar{n}/k)^{n+k}} \qquad (5)$$

are given in table 6. In this two-parameter fit, the energy dependence of the parameter $1/k$ as well as its comparison to e^+e^-, lh and non-diffractive hh interactions are of special interest. This is shown in fig. 9. The dashed line for $pp/p\bar{p}$ therein represents the linear $ln\sqrt{s}$ dependence fitted in [24] and the solid line is the linear fit to e^+e^- results at $\sqrt{s} > 4$ GeV done in [16]. The experimental points for $\bar{\nu}p$ interactions are taken from [19b], for μ^+p reactions from [19d] and for M^+p data from [16, 21a,b,c,e] where M^+ denotes positively charged mesons. All reaction types give $1/k$-values rising with energy.

Above 6 GeV, the diffractive, lepton-hadron and meson-hadron data lie between the two lines for $pp/p\bar{p}$ and e^+e^- interactions in accordance with the findings for the energy dependence of the ratio $<n_{ch}^D>/D$ (see fig. 5) and not in contradiction to the behaviour of the KNO-parameter c (see fig. 8).

4 Summary

The multiplicity structure of meson and proton diffraction in π^+/K^+p interactions at 250 GeV/c is investigated and compared to hadron production in e^+e^-, lh and non-diffractive hh reactions. The main results are:

(i) Except for the lowest mass the average charge multiplicity for meson diffraction is significantly larger than that for proton diffraction, a difference also observed between non-diffractive meson-proton and proton-proton interactions. Their energy dependence can be well fitted with a polynomial quadratic in $ln\,M_D$ where M_D is the diffractive mass.

(ii) With increasing energy the multiplicity distribution for meson diffraction is getting narrower than that for proton diffraction, again resembling non-diffractive hadron-hadron interactions.

(iii) The energy dependence of the average multiplicity for meson diffraction is compatible with that for e^+e^- collisions and that for proton diffraction compatible with that for μ^+p and $\bar{\nu}p$ scattering. However, systematic differences are revealed when studying the shape of the multiplicity distributions in more detail.

(iv) From an analysis of the energy dependence of diffractive multiplicity distributions in terms of the ratio $< n_{ch} > /D$, their KNO-form and a Negative Binomial parametrization and a comparison of the results with those from e^+e^-, lh and non-diffractive hh interactions, the following picture is suggested at sufficiently high energies: e^+e^- and $pp/p\bar{p}$ data set the limits for the variation of the parameters investigated. Diffractive, lp and meson-proton data lie between these limits. Data at higher energies for diffraction and lp reactions are needed to be still more specific.

Acknowledgements: We are indebted to the CERN SPS, beam and EHS crews for their support during the runs for our experiment. It is a pleasure to thank the scanning and measuring staffs of our laboratories. The contributions of the groups at Aachen, Helsinki and Warsaw to the earlier phase of this experiment are highly appreciated.

References

[1] M.Adamus et al. (NA22), Z.Phys. C39 (1988) 301.

[2] R.Bonino et al. (UA8), Phys.Lett. B 211 (1988) 239.

[3] M.Asai et al. (NA23), Z.Phys. C46 (1990) 593.

[4] P.Schlein et al. (UA8), Hard Diffraction and Double Pomeron Exchange in UA8, Proc. of the Joint International Lepton- Photon Symposium & Europhysics Conference on High Energy Physics, Geneva (1991), p.

[5] H.Böttcher et al. (NA22), New Results on Meson Diffraction in π^+/K^+p Interactions at 250 GeV/c, Proc. of the Joint International Lepton-Photon Symposium & Europhysics Conference on High Energy Physics, Geneva (1991), p.

[6] I.V.Ajinenko et al. (NA22), "Study of Internal. Structure of Meson Diffractive Systems in π^+p and K^+p Interactions at 250 GeV/c", to be submitted to Z.Phys. C.

[7] A.Donnachie and P.V.Landshoff, Nucl.Phys. B244 (1984) 322.

[8] G.Ingelman, Proc.Workshop on Elastic and Diffractive Scattering at the Collider and Beyond, Chateau de Blois (1985), p.

[9] G.Ingelman and P.Schlein, Phys.Lett. B152 (1985) 256.

[10] B.Andersson et al., LUND-Univ. preprint LU-TP 87-6 (1987).

[11] G.Ingelman, Soft processes in very high energy proton-proton collisions, DESY-preprint 88-014 (1988).

[12] J.Dias de Deus, Phys.Lett. B216 (1989) 431.

[13] V.Innocente et al., Phys.Lett. B169 (1986) 285.

[14] J.Ranft, Z.Phys. C33 (1987) 517.

[15] A.B.Kaidalov and K.A.Ter-Martirosyan, Phys.Lett. B117 (1982) 247.

[16] M.Adamus et al., Z.Phys. C32 (1986) 475.

[17] NA22 Collaboration: Charge and Strangeness Flow in Diffraction Dissociation of π^+ and K^+ Mesons at 250 GeV/c, in preparation.

[18] a) J.L.Siegrist et al. (MARK I), Phys.Rev. D26 (1982) 969.
b) B.Niczyporuk et al. (LENA), Z.Phys. C9 (1981) 1.
c) Ch.Berger et al. (PLUTO), Phys.Lett. B95 (1980) 313.
d) W.Bartel et al. (JADE), Z.Phys. C20 (1983) 187.
e) M.Althoff et al. (TASSO), Z.Phys. C22 (1984) 307.
f) M.Derrick (HRS), ANL-HEP-CP-86-26.
g) M.S.Alam et al. (CLEO), Phys.Rev.Lett. 49 (1982) 357.
h) R.Hollebeek (MARK II), Int.Symp.Lepton and Photon Int., Bonn, 1981.

[19] a) H.Grässler et al. (BEBC), Nucl.Phys. B223 (1983) 269.
b) B.Jongejans et al. (BEBC), Nuov.Cim. 101A (1989) 435.
c) M.Arneodo et al. (EMC), Nucl.Phys. B258 (1985) 249.
d) M.Arneodo et al. (EMC), Z.Phys. C35 (1987) 335.

[20] a) H.W.Zheng et al. (AMY), Phys.Rev. D42 (1990) 737.
b) P.Abreu et al. (DELPHI), Z.Phys. C50 (1991) 185.

[21] a) G.A.Akopdjanov et al., Nucl.Phys. B75 (1974) 401.
b) C.Bromberg et al., Phys.Rev. D15 (1977) 64.
c) W.M.Morse et al., Phys.Rev. D15 (1977) 66.
d) G.Ransone et al., Nucl.Phys. B167 (1980) 285.
e) D.Brick et al., Phys.Rev. D25 (1982) 2794.

[22] W.Thome et al., Nucl.Phys. B129 (1977) 365.

[23] D.Levy, Nucl.Phys. B59 (1973) 583.

[24] G.J.Alner et al., Phys.Lett. B160 (1985) 199, B167 (1986) 476.

TABLE 1

Fit of the average charge multiplicity $< n_{ch}^{D} >$ of meson (π_D^+/K_D^+) and proton (p_D) diffraction as function of the diffractive mass M_D or the available energy E_a in π^+/K^+p interactions at $250\,GeV/c$.

	x	Energy Range, GeV	$< n_{ch}^{D} > = A + B\,lnx + C\,ln^2x$			
			A	B	C	χ^2/NDF
π_D^+/K_D^+	M_D	1.0 - 8.4	2.04 ± 0.09	0.32 ± 0.22	0.76 ± 0.11	8.1 / 6
	E_a	1.0 - 8.3	2.05 ± 0.10	0.67 ± 0.23	0.59 ± 0.13	2.7 / 6
p_D	M_D	1.0 - 9.7	2.34 ± 0.14	-0.89 ± 0.24	1.06 ± 0.10	4.0 / 7
	E_a	1.0 - 8.8	2.20 ± 0.15	0.10 ± 0.30	0.67 ± 0.15	3.8 / 6

TABLE 2

Multiplicity moments for meson diffraction in π^+/K^+p interactions at $250\,GeV/c$ as function of the diffractive mass M_D.

$< M_D >$, GeV	$< n_{ch}^{D} >$	D	$< n_{ch}^{D} > /D$	f_2
1.20	2.18 ± 0.07	1.11 ± 0.08	1.97 ± 0.16	-0.95 ± 0.07
1.74	2.37 ± 0.07	1.18 ± 0.07	2.01 ± 0.13	-0.98 ± 0.07
2.29	2.75 ± 0.07	1.36 ± 0.12	2.02 ± 0.19	-0.91 ± 0.07
2.75	3.25 ± 0.08	1.40 ± 0.13	2.32 ± 0.22	-1.28 ± 0.08
3.31	3.59 ± 0.09	1.40 ± 0.13	2.56 ± 0.25	-1.64 ± 0.09
3.98	3.96 ± 0.09	1.63 ± 0.17	2.43 ± 0.26	-1.31 ± 0.09
4.79	4.31 ± 0.14	1.73 ± 0.18	2.49 ± 0.27	-1.33 ± 0.14
5.75	5.04 ± 0.14	2.01 ± 0.27	2.51 ± 0.34	-0.99 ± 0.15
7.35	5.52 ± 0.18	2.24 ± 0.30	2.46 ± 0.34	-0.51 ± 0.20

TABLE 3

Multiplicity moments for proton diffraction in π^+/K^+p interactions at $250\,GeV/c$ as function of the diffractive mass M_D.

$< M_D >$, GeV	$< n_{ch}^D >$	D	$< n_{ch}^D > / D$	f_2
1.20	2.23 ± 0.12	1.43 ± 0.26	1.56 ± 0.30	-0.19 ± 0.14
1.74	2.16 ± 0.10	1.11 ± 0.10	1.95 ± 0.20	-0.93 ± 0.10
2.29	2.27 ± 0.09	1.27 ± 0.13	1.79 ± 0.20	-0.66 ± 0.09
2.75	2.60 ± 0.07	1.33 ± 0.11	1.95 ± 0.17	-0.83 ± 0.07
3.31	2.70 ± 0.07	1.35 ± 0.12	2.00 ± 0.19	-0.89 ± 0.07
3.98	3.16 ± 0.07	1.53 ± 0.13	2.07 ± 0.18	-0.83 ± 0.07
4.79	3.55 ± 0.08	1.66 ± 0.16	2.14 ± 0.21	-0.81 ± 0.08
5.75	4.04 ± 0.11	1.92 ± 0.21	2.10 ± 0.24	-0.37 ± 0.12
6.92	4.45 ± 0.21	2.14 ± 0.29	2.08 ± 0.30	+0.14 ± 0.23
8.65	5.33 ± 0.16	2.43 ± 0.58	2.19 ± 0.33	+0.58 ± 0.21

TABLE 4

Multiplicity distributions for meson diffraction in π^+/K^+p interactions at $250\,GeV/c$ in terms of probabilities $P_{n_{ch}}$ for various intervals of the diffractive mass M_D.

n_{ch}^D	$< M_D >$, GeV				
	3.3	4.0	4.8	5.8	7.4
1	0.094 ± 0.014	0.084 ± 0.014	0.060 ± 0.011	0.020 ± 0.008	0.020 ± 0.006
3	0.560 ± 0.044	0.453 ± 0.037	0.399 ± 0.032	0.304 ± 0.026	0.237 ± 0.023
5	0.304 ± 0.030	0.380 ± 0.033	0.396 ± 0.032	0.421 ± 0.031	0.374 ± 0.031
7	0.039 ± 0.009	0.063 ± 0.012	0.121 ± 0.016	0.173 ± 0.020	0.245 ± 0.024
9	0.002 ± 0.002	0.021 ± 0.007	0.023 ± 0.007	0.056 ± 0.011	0.092 ± 0.014
11			0.001 ± 0.001	0.026 ± 0.008	0.023 ± 0.007
13					0.008 ± 0.004
15					0.002 ± 0.002

TABLE 5

Multiplicity distributions for proton diffraction in π^+/K^+p interactions at $250\,GeV/c$ in terms of probability $P_{n_{ch}}$ for various intervals of the diffractive mass M_D.

n_{ch}^D	$< M_D >, GeV$					
	3.3	4.0	4.8	5.8	6.9	8.7
1	0.308 ± 0.029	0.205 ± 0.020	0.161 ± 0.017	0.129 ± 0.015	0.099 ± 0.015	0.051 ± 0.014
3	0.540 ± 0.041	0.556 ± 0.036	0.479 ± 0.034	0.400 ± 0.030	0.357 ± 0.031	0.281 ± 0.059
5	0.147 ± 0.019	0.196 ± 0.019	0.285 ± 0.024	0.316 ± 0.026	0.336 ± 0.030	0.302 ± 0.063
7	0.005 ± 0.003	0.039 ± 0.008	0.071 ± 0.011	0.131 ± 0.015	0.158 ± 0.019	0.223 ± 0.048
9		0.004 ± 0.003	0.004 ± 0.003	0.023 ± 0.006	0.028 ± 0.008	0.115 ± 0.027
11				0.001 ± 0.001	0.023 ± 0.007	0.018 ± 0.007
13						0.005 ± 0.003
15						0.004 ± 0.003

TABLE 6

Results of KNO and Neg.Bin. fits to the multiplicity distribution in different mass intervals for meson (π_D^+/K_D^+) and proton (p_D) diffraction in π^+/K^+p interactions at $250\,GeV/c$ (For the parametrization see text).

	$< M_D >$, GeV	KNO - FIT		NEG.-BIN.-FIT		
		c	χ^2/NDF	$\bar{n}$	$1/k$	χ^2/NDF
π_D^+/K_D^+	3.3	6.57 ± 0.43	0.1 / 4	3.60 ± 0.07	-0.124 ± 0.011	5.4 / 3
	4.0	6.29 ± 0.46	7.5 / 4	3.88 ± 0.07	-0.105 ± 0.012	8.8 / 3
	4.8	6.29 ± 0.40	0.7 / 5	4.31 ± 0.08	-0.072 ± 0.011	4.6 / 4
	5.8	7.34 ± 0.49	13.6 / 5	4.97 ± 0.11	-0.066 ± 0.012	23.6 / 4
	7.4	6.76 ± 0.41	5.2 / 7	5.53 ± 0.10	-0.031 ± 0.010	9.0 / 6
p_D	3.3	4.36 ± 0.31	2.3 / 3	2.68 ± 0.07	-0.115 ± 0.015	0.6 / 2
	4.0	4.09 ± 0.31	1.3 / 4	3.14 ± 0.07	-0.077 ± 0.018	8.6 / 3
	4.8	4.70 ± 0.28	1.9 / 4	3.55 ± 0.07	-0.064 ± 0.012	1.1 / 3
	5.8	4.56 ± 0.25	3.0 / 5	4.03 ± 0.08	-0.027 ± 0.012	2.2 / 4
	6.9	4.79 ± 0.36	8.7 / 5	4.36 ± 0.10	-0.015 ± 0.016	8.3 / 4
	8.7	5.10 ± 0.31	8.3 / 7	5.29 ± 0.11	+0.011 ± 0.012	8.5 / 6

Figure captions

Fig.1: Average charge multiplicity of meson and proton diffraction as function of the diffractive mass M_D (fig. 1a) and the available energy E_a (fig.1b). The lines are fits of polynomials quadratic in $ln\ M_D$ and $ln\ E_a$, respectively.

Fig.2: The dispersion D, the ratio $<n_{ch}^D> /D$ and the correlation parameter f_2 of the multiplicity distribution for meson (fig. 2a, c,e) and proton (fig. 2b,d,f) diffraction as function of the diffractive Mass M_D.

Fig.3: Energy dependence of the average charge multiplicity of meson diffraction compared to e^+e^- data.

Fig.4: Energy dependence of the average charge multiplicty of proton diffraction compared to lepton-hadron data.

Fig.5: The ratio $<n_{ch}^D> /D$ as function of the energy for meson and proton diffraction and compared with e^+e^- , μ^+p and non-diffractive hh data. The dashed lines are only to guide the eye.

Fig.6: Multiplicity distributions in KNO-form for meson diffraction (full symbols) compared to e^+e^- data. The lines represent fits to these data according to the parametrization (4) separately for meson diffraction (full line) and e^+e^- collisions (dashed line).

Fig.7: Multiplicity distributions in KNO-form for proton diffraction (full symbols) compared to μ^+p data. The lines represent fits to these data according to the parametrization (4) separately for proton diffraction (full line) and μ^+p interactions (dashed line).

Fig.8: Energy dependence for the KNO-parameter c for meson (fig. 8a) and proton (fig.8b) diffraction compared to e^+e^- and lp data.

Fig.9: Energy dependence of $1/k$-parameter of the Negative Binomial distribution fitted to meson and proton diffraction and compared to e^+e^- , lp and non-diffractive hh data.

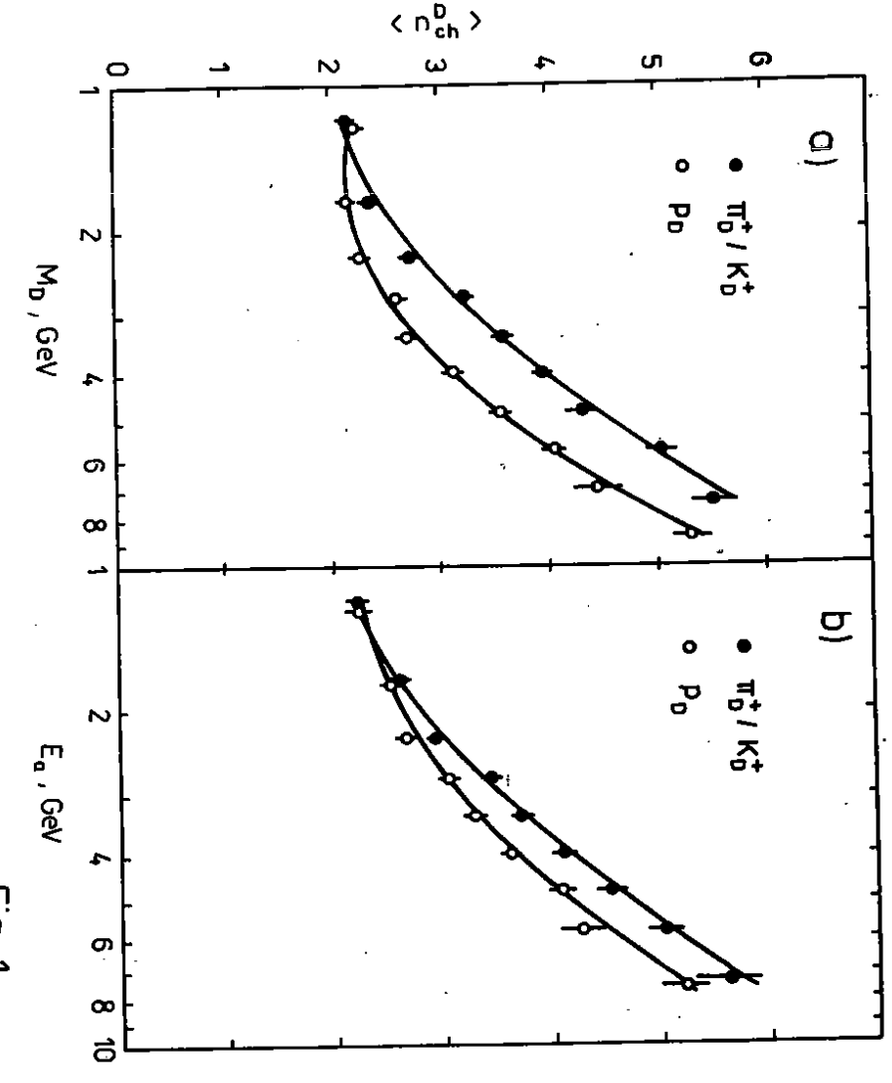

Fig.1

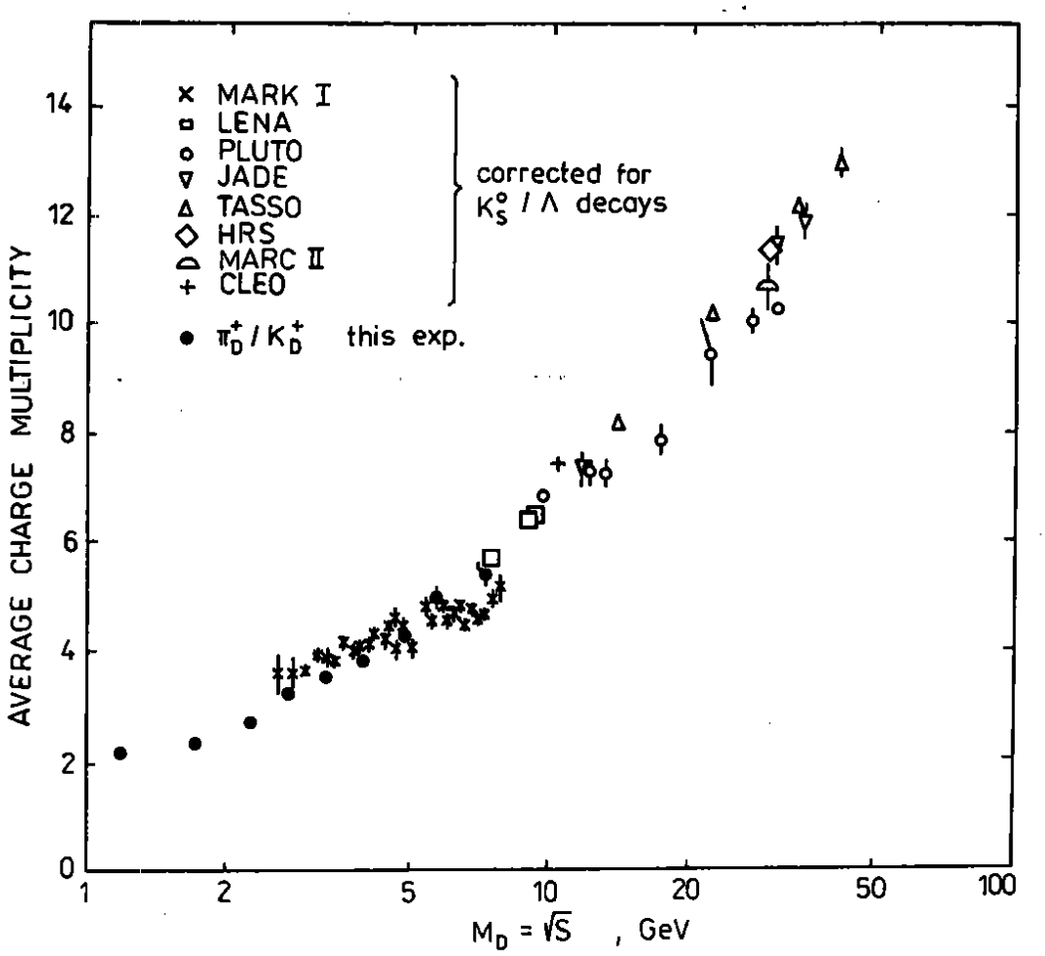
MARK I
LENA
PLUTO
JADE
TASSO
HRS
MARC II
CLEO
corrected for
K_S^0 / Λ decays
π_D^+ / K_D^+ this exp.
AVERAGE CHARGE MULTIPLICITY
$M_D = \sqrt{S}$, GeV

Fig. 3

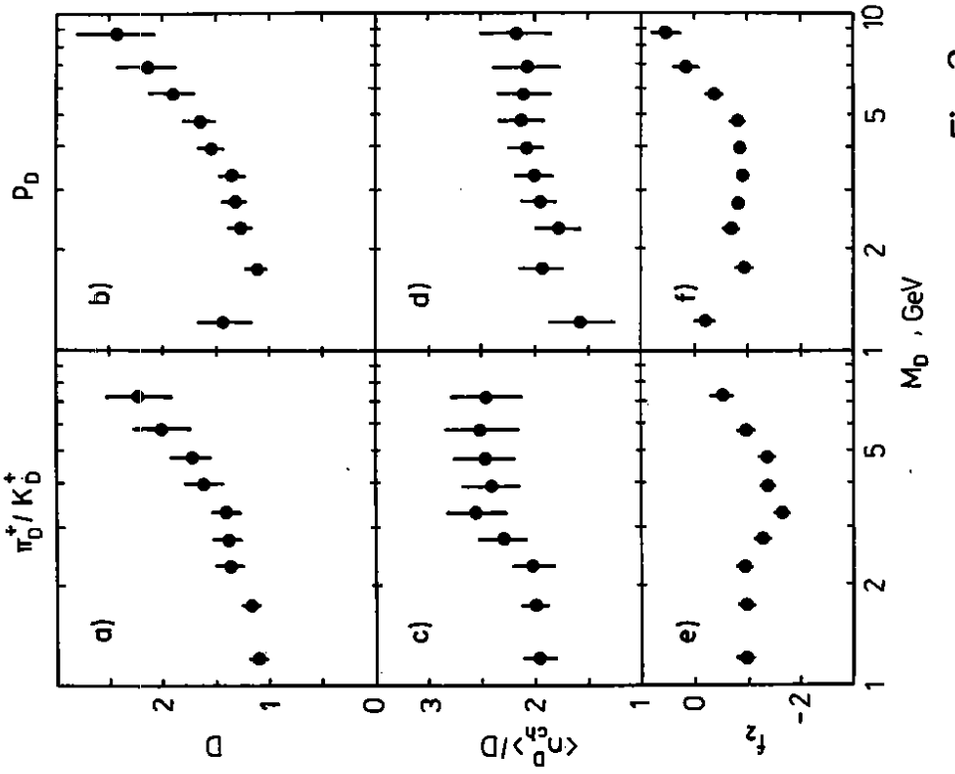
P_D
π_D^+ / K_D^+
D
$\langle n_{ch}^D \rangle / D$
f_2
M_D , GeV
a)
b)
c)
d)
e)
f)

Fig. 2

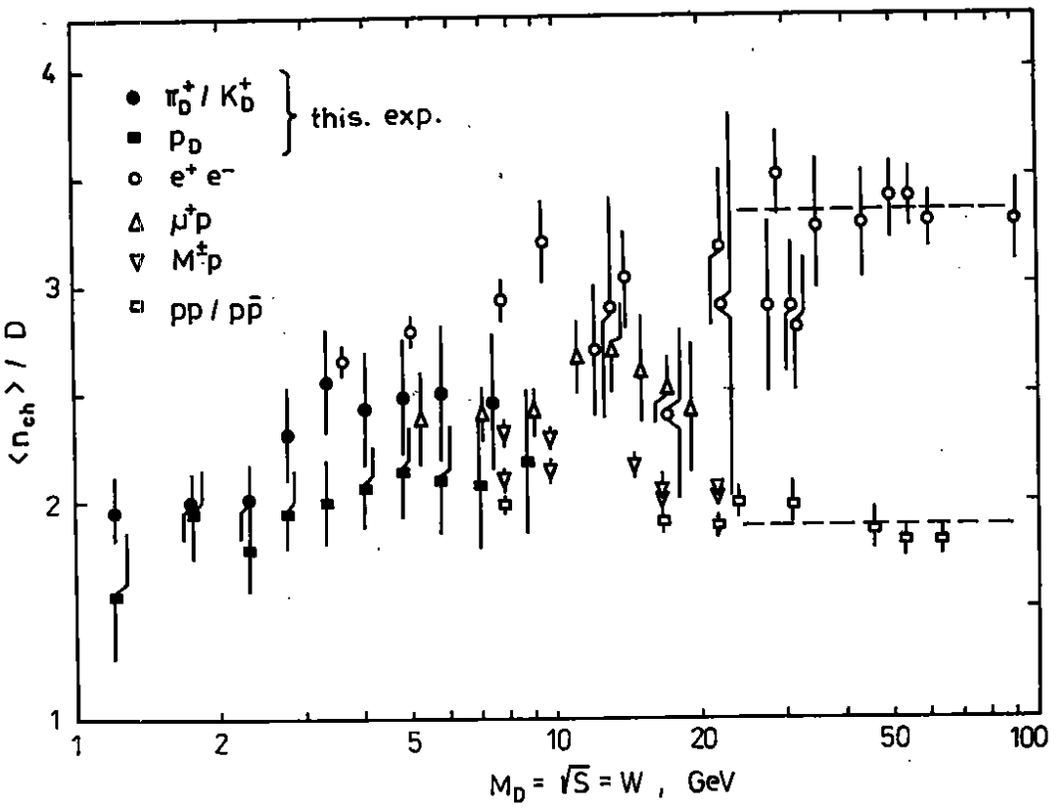
π_D^+ / K_D^+
p_D
$e^+ e^-$
$\mu^+ p$
$M^\pm p$
$pp / p\bar{p}$
this. exp.
$\langle n_{ch} \rangle / D$
$M_D = \sqrt{S} = W$, GeV

Fig. 5

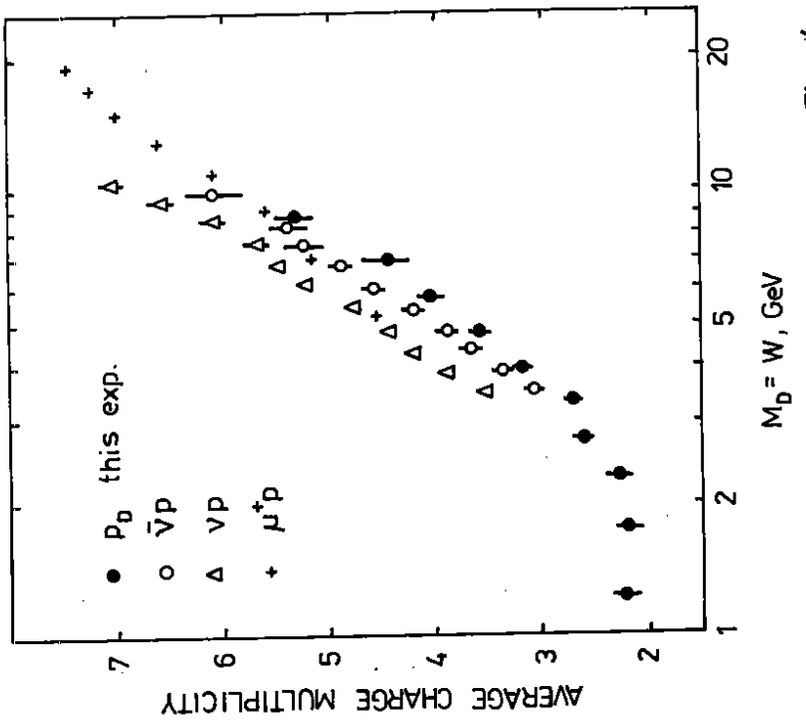
p_D this exp.
$\bar{\nu} p$
νp
$\mu^+ p$
AVERAGE CHARGE MULTIPLICITY
$M_D = W$, GeV

Fig. 4

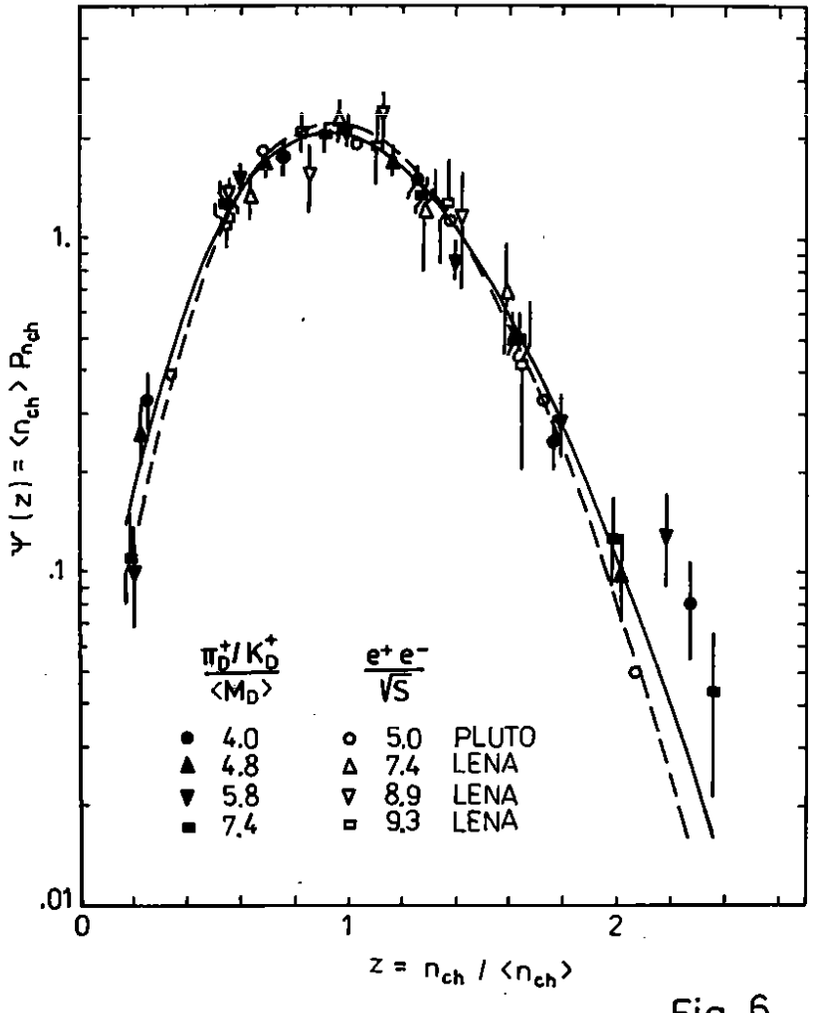
Ψ (z) = ⟨n_ch⟩ P_nch
1.
.1
.01
0
1
2
z = n_ch / ⟨n_ch⟩
π_D^+ / K_D^+
⟨M_D⟩
e^+ e^-
√S
4.0
4.8
5.8
7.4
5.0 PLUTO
7.4 LENA
8.9 LENA
9.3 LENA

Fig.6

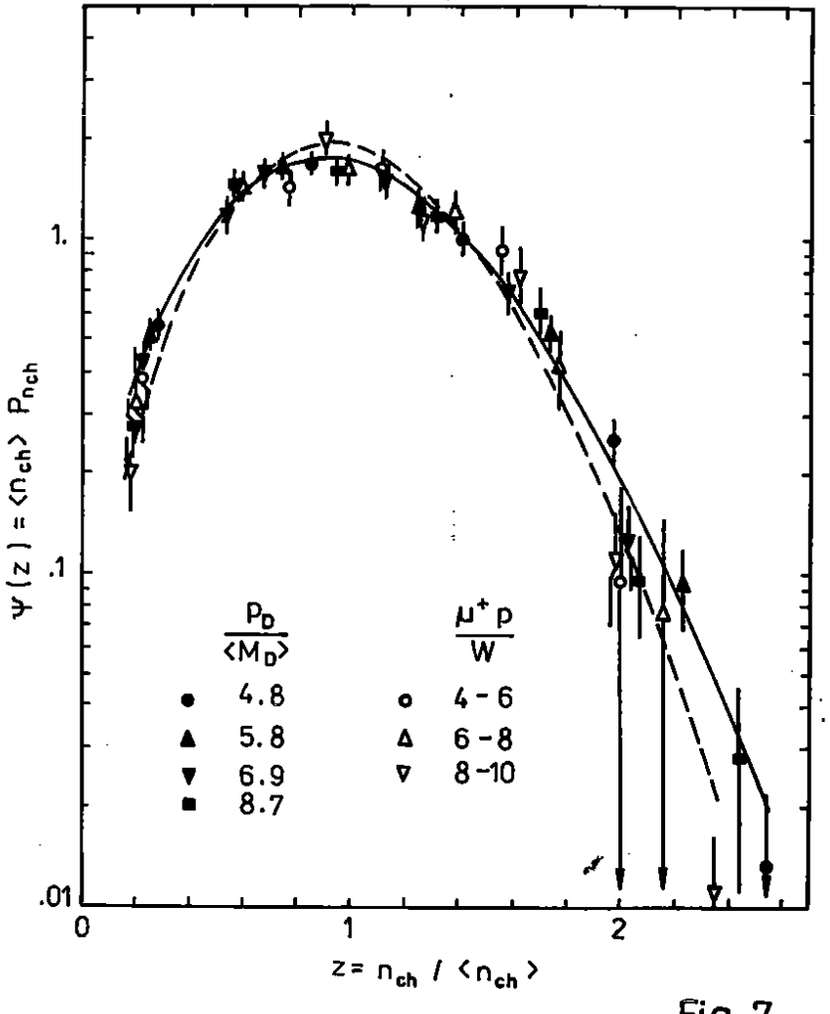
Ψ (z) = ⟨n_ch⟩ P_nch
1.
.1
.01
0
1
2
z = n_ch / ⟨n_ch⟩
P_D
⟨M_D⟩
μ^+ p
W
4.8
5.8
6.9
8.7
4 - 6
6 - 8
8 - 10

Fig.7

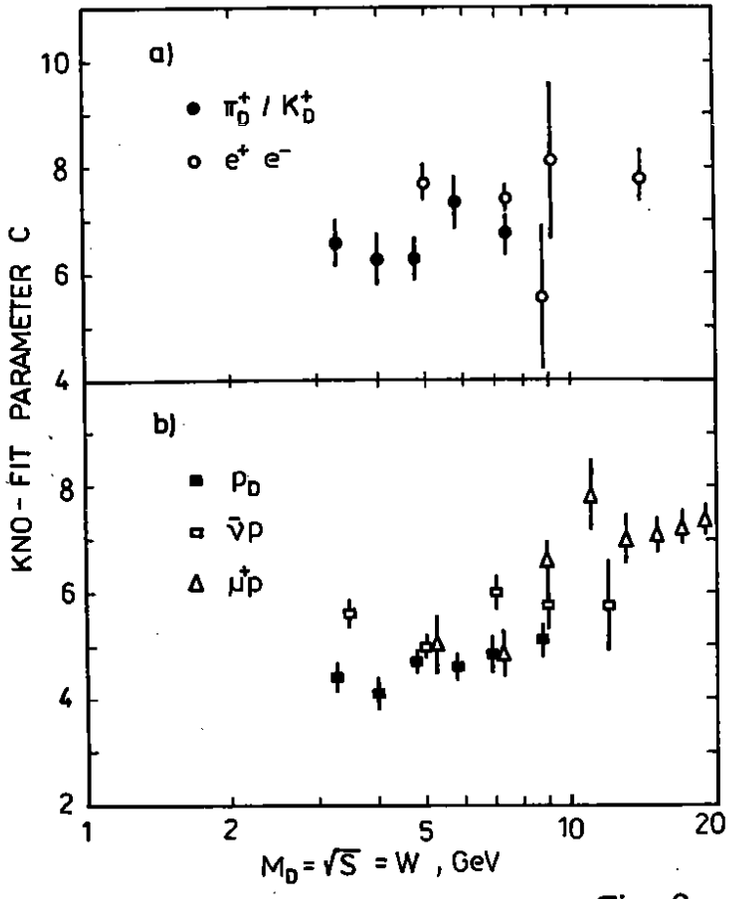
a)
π_D^+ / K_D^+
$e^+ e^-$
b)
p_D
$\bar{\nu} p$
$\mu^+ p$
KNO - FIT PARAMETER C
$M_D = \sqrt{S} = W$, GeV

Fig. 8

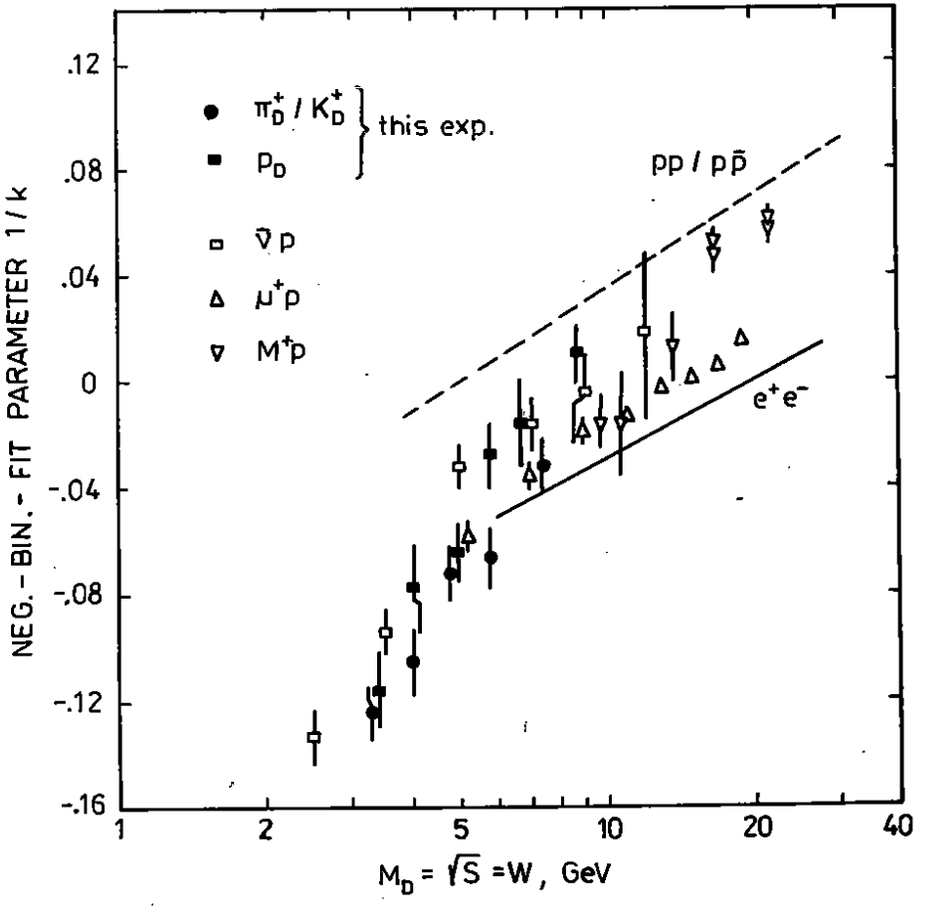
π_D^+ / K_D^+
this exp.
p_D
$\bar{\nu} p$
$\mu^+ p$
$M^+ p$
$pp / p\bar{p}$
$e^+ e^-$
NEG. - BIN. - FIT PARAMETER 1 / k
$M_D = \sqrt{S} = W$, GeV

Fig. 9